

Three-level quantum amplifier as a heat engine: A study in finite-time thermodynamics

Eitan Geva and Ronnie Kosloff

Department of Physical Chemistry and the Fritz Haber Research Center, The Hebrew University, Jerusalem 91904, Israel

(Received 8 November 1993)

The finite-rate performance of a quantum heat engine, constructed from a three-level amplifier, is analyzed. Consistent definitions of thermodynamical quantities in terms of quantum observables are postulated. The performance is analyzed in steady state, where the operation of the amplifier only influences the surroundings. Quantum master equations describe the irreversible dynamics induced by the coupling of the working medium to the reservoirs. It is shown that the standard assumption of field-independent dissipation is inconsistent with thermodynamics. Field-dependent relaxation equations, based upon the semigroup approach, and consistent with thermodynamics, are formulated. These equations are valid if the time scale of the external field is slow compared to that associated with the bath fluctuations. The steady-state values of the thermodynamical quantities are evaluated. The power is found to have maxima as a function of important controls, such as the field amplitude, frequency, and the coupling with the baths. The existence and locations of these maxima differ from those obtained in the standard treatment, where the dissipation is field independent. The irreversible nature of engine operation is due to the finite rate of heat transfer and a genuine "quantum-friction" loss term due to dephasing.

PACS number(s): 05.30.-d, 42.50.-p

I. INTRODUCTION

The study of heat engines constitutes a crucial bridge between abstract theory and realizable physical phenomena. It was Carnot's concept of the heat engine which first linked the second law of thermodynamics with the upper bound on the efficiency of steam engines [1]. More recently, macroscopic transport theory has been linked with thermodynamics to provide more realistic upper bounds on the performance of finite-rate thermodynamical processes. "Finite-time thermodynamics" is the new field of research that emerged from such studies. It is concerned with optimizing the performance of processes subject to constraints of finite duration or rate [2]. Finite-time thermodynamics combines three disciplines: thermodynamics, which traditionally lacks the time dimension, transport dynamics, and optimal control theory.

All previous studies in this field (with the exception of Refs. [3-5]) based the underlying dynamics on a transport theory which is applicable in the classical regime, i.e., macroscopic systems at high temperature. For example, the effect of dephasing, which is of fundamental importance for the quantum engine, is absent. The objective of this study is to understand the implications of quantum dynamics on the performance of heat engines. To obtain this goal the dynamics have to be based on the quantum theory of open systems. Consistent definitions of thermodynamical quantities in terms of quantum observables should then be postulated. This setup constitutes the bridge between quantum theory and thermodynamics.

The main obstacle is the lack of a closed theory for the relaxation dynamics of systems interacting with intense

time-dependent external fields. The relaxation dynamics is independent of the external field in the common approach, which corresponds to the limit of weak fields [6]. It will be shown that in order to be consistent with thermodynamics the dissipation must be field dependent. The demand for consistency with thermodynamics is the guide to the construction of simplified field-dependent relaxation equations. These equations are valid when the time scale of the external field is slow compared to that of the bath fluctuations. The analysis provided here is restricted to the effect of nondiagonal coupling with the heat reservoirs, where the nondiagonality is with respect to the energy representation. Thus the results obtained provide the performance limitations originating from one source of irreversibility, associated with nondiagonal coupling. The neglect of diagonal coupling has the advantage of considerably simplifying the model, allowing a straightforward interpretation of the results. This approach towards the dynamics has two other advantages: it is based upon a microscopic dynamical theory and is therefore more fundamental, and it is valid outside the vicinity of equilibrium.

In the present work a quantum heat engine is the subject of study. The model is based on a three-level amplifier which can be realized as a heat engine [7]. The present model differs from previously studied models of quantum heat engines [3,4] in the following respects.

(a) Previous models treated four stroke engines of the Carnot type. The working medium consisted of non-interacting spin- j atoms or harmonic oscillators. In each stroke of the engine the working medium interacts with one or none of the two heat reservoirs. The engine then produces a net amount of work per cycle. The present

quantum engine, on the other hand, uses a continuous mode of operation. This means that each of the reservoirs is coupled to different degrees of freedom of the working medium, simultaneously. In steady state the rate of heat absorption from the hot reservoir is equal to the net rate of heat dissipated into the cold reservoir and work performed on the work reservoir.

(b) The only source of irreversibility in previous models was due to the finite rate of heat transfer between the working medium and the heat reservoirs. The present model contains an additional source of irreversibility which resides in the coupling to the work reservoir. This source may be interpreted as a genuine type of “quantum friction.” It is due to the fact that the total Hamiltonian of the working medium does not commute with the interaction term between the working medium and the work reservoir.

The irreversible operation of the amplifier is studied, in the spirit of finite-time thermodynamics. It is shown that the power output has maxima with respect to all important control variables: the external field amplitude and frequency, the heat reservoirs’ temperatures, and the coupling of the working medium with the heat reservoirs.

The performance of the amplifier was compared to that of Lamb’s semiclassical model of the three-level laser [8], where the relaxation is field independent. Therefore the deviations from Lamb’s model are due to the influence of the time-dependent external field on the relaxation, included in the present model. In particular, power production will eventually decrease for intense fields, due to nonlinear effects residing in the relaxation terms.

The basic model describing the relation between the three-level amplifier and the heat engine is presented in Sec. II. The linkage between thermodynamical quantities and quantum observable is discussed in Sec. III. The conditions for steady state operation are described in Sec. IV. The dynamics of quantum open systems in terms of quantum master equations are described in Sec. V. The thermodynamic inconsistency associated with the assumption of field-independent relaxation is demonstrated in Sec. VI. The formulation of field-dependent relaxation equations, consistent with thermodynamics, is described in Sec. VII. The relaxation equations are solved for the steady state values of the thermodynamical quantities, in Sec. VIII. The optimization of power output with respect to the controls is described in Sec. IX. A discussion of the results and their relation to previous work is presented in Sec. X.

II. THE BASIC MODEL

A generic heat engine [9] consists of four components: the working medium, the power output mechanism, and the hot and cold reservoirs, cf. Fig. 1. In order to model quantum engines, the quantum realization of these components must be pointed out. For the case of the quantum three-level amplifier these four components are modeled in the following manner [7].

(a) The working medium consists of many non-interacting three-level atoms. For the sake of simplicity,

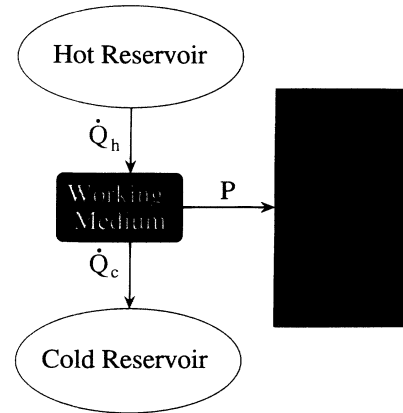


FIG. 1. The generic heat engine. The arrows indicate the directions of the heat and work currents.

the unperturbed energy levels are equispaced. The unperturbed levels in order of increasing energy are $-\omega_0$, 0 , and ω_0 ($\omega_0 > 0$ and $\hbar = 1$). The Hamiltonian of a single unperturbed three-level atom is given by

$$\mathbf{H}_0 = \omega_0(\mathbf{P}_1 - \mathbf{P}_{-1}), \quad (2.1)$$

where $\mathbf{P}_i \equiv \mathbf{P}_{ii} \equiv |i\rangle\langle i|$ are the projection operators defined by the eigenvectors $|-1\rangle$, $|0\rangle$ and $|1\rangle$ of \mathbf{H}_0 , corresponding to the eigenvalues $-\omega_0$, 0 , and ω_0 , respectively.

(b) The power output mechanism is modeled by coupling the two uppermost energy levels of each atom (i.e., $|0\rangle$ and $|1\rangle$), with a classical monochromatic electromagnetic field of circular polarization. The interaction between the field and the atom is represented by the following time-dependent Hamiltonian:

$$\mathbf{H}_I = \epsilon(e^{-i\omega t}\mathbf{P}_{1,0} + e^{i\omega t}\mathbf{P}_{0,1}), \quad (2.2)$$

where $\mathbf{P}_{i,j} \equiv |i\rangle\langle j|$, ω is the field frequency, and ϵ is a parameter representing the strength of the coupling between the system and the external field. ϵ is proportional to the field’s amplitude and will be referred to as “the field’s amplitude” in the rest of this paper.

(c) The thermal coupling to the reservoirs is modeled by quantum master equations [10]. The hot reservoir of temperature T_h is coupled to the transition between the extreme energy levels corresponding to $|-1\rangle$ and $|1\rangle$. The cold reservoir of temperature T_c is coupled to the two lowest energy levels corresponding to $|-1\rangle$ and $|0\rangle$ (cf. Fig. 2). Obviously $T_h > T_c > 0$. The temperatures in the rest of this paper are measured in energy units.

Summarizing all the contributions to the dynamics, the equation of motion of the observable becomes, in the Heisenberg picture,

$$\dot{\mathbf{X}} = i[\mathbf{H}, \mathbf{X}] + \frac{\partial \mathbf{X}}{\partial t} + \mathcal{L}_D^h(\mathbf{X}) + \mathcal{L}_D^c(\mathbf{X}). \quad (2.3)$$

\mathbf{X} is an arbitrary operator from the Hilbert space of the atom. The first term on the right-hand side of Eq. (2.3) is due to the evolution induced by the total Hamiltonian, $\mathbf{H} = \mathbf{H}_0 + \mathbf{H}_I$. The second term on the right-hand

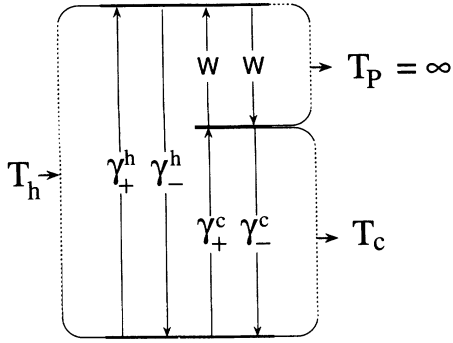


FIG. 2. The three-level quantum amplifier as a heat engine. γ_+^h , γ_-^h , γ_+^c , and γ_-^c are the thermal transition probabilities, and W is the field-induced transition probability. In steady state, the heat absorbed from the hot reservoir of temperature T_h is transformed into induced emission (work) which amplifies the external field, and heat is dumped into the cold reservoir of temperature T_c . The horizontal arrows indicate the direction of the energy fluxes.

side corresponds to the time evolution due to a possible explicit time dependence of the operator \mathbf{X} . The last two terms on the right-hand side, $\mathcal{L}_D^h(\mathbf{X})$ and $\mathcal{L}_D^c(\mathbf{X})$, represent the dissipative evolution, induced by the coupling with the hot and cold reservoirs, respectively. The explicit form of these terms will be discussed in Secs. V-VII.

The heat engine realization described above functions as an amplifier in the following manner (cf. Fig. 2): the selective thermal coupling to sufficiently hot and cold reservoirs maintains a steady population inversion between the two uppermost levels. Net induced emission is obtained which adds to the external field, and amplifies it. Since the coupling with the external world is via a field of frequency ω , the radiation emitted is of the same frequency. The model assumes that the amplified radiation does not react back on the atom. This corresponds to a semiclassical approximation with respect to the atom-field interaction [11].

III. THERMODYNAMIC RELATIONS

Thermodynamic expressions are obtained by substituting a thermodynamic observable for the operator \mathbf{X} in Eq. (2.3). In particular, the change in energy is obtained by substituting the Hamiltonian \mathbf{H} for \mathbf{X} . Since the Hamiltonian commutes with itself the change in energy of the system simplifies to

$$\frac{dE}{dt} \equiv \langle \dot{\mathbf{H}} \rangle = \left\langle \frac{\partial \mathbf{H}}{\partial t} \right\rangle + \langle \mathcal{L}_D^h(\mathbf{H}) \rangle + \langle \mathcal{L}_D^c(\mathbf{H}) \rangle. \quad (3.1)$$

Equation (3.1) is the time derivative of the first law of thermodynamics [3-5,12,13]. The instantaneous power is identified as

$$\mathcal{P} \equiv \left\langle \frac{\partial \mathbf{H}}{\partial t} \right\rangle = \left\langle \frac{\partial \mathbf{H}_I}{\partial t} \right\rangle = -i\epsilon\omega(e^{-i\omega t}\langle \mathbf{P}_{1,0} \rangle - e^{i\omega t}\langle \mathbf{P}_{0,1} \rangle), \quad (3.2)$$

and the instantaneous heat fluxes are identified as

$$\dot{Q}_h \equiv \langle \mathcal{L}_D^h(\mathbf{H}) \rangle, \quad \dot{Q}_c \equiv \langle \mathcal{L}_D^c(\mathbf{H}) \rangle. \quad (3.3)$$

The engine in this study is operated under steady-state conditions. This mode of operation is obtainable due to the interplay between the relaxation processes and the power output mechanism. Under steady-state operation conditions the energy of the working medium is constant. Energy conservation then assumes the form of Kirchoff's law: the sum of fluxes to the engine is zero,

$$\mathcal{P} + \dot{Q}_c + \dot{Q}_h = 0. \quad (3.4)$$

Entropy production in steady state is given by

$$\sigma = -\beta_c \dot{Q}_c - \beta_h \dot{Q}_h, \quad (3.5)$$

where $\beta_c \equiv 1/T_c$ and $\beta_h \equiv 1/T_h$ are the inverse temperatures of the cold and hot reservoirs, respectively. The steady-state entropy of the working medium is constant, and entropy is only being generated in the heat reservoirs. Finally, the steady-state thermodynamic efficiency of the amplifier is defined as the ratio of the power obtained to the heat flux absorbed from the hot reservoir:

$$\eta = -\frac{\mathcal{P}}{\dot{Q}_h} = 1 + \frac{\dot{Q}_c}{\dot{Q}_h}. \quad (3.6)$$

IV. THE STEADY-STATE OPERATION IN THE ROTATING FRAME

The explicit time dependence of the generator of motion in the continuous heat engine model [Eq. (2.3)] originates in the interaction with a periodic field. This field has a single frequency component of frequency ω . Thus, according to the Floquet theorem, the time dependence of the system's observables becomes periodic, with a period of $2\pi/\omega$. To exploit this property, it is advantageous to change to a reference frame rotating with a frequency ω [6,11].

The rotating frame is defined, in terms of the Schrödinger picture, by the following transformation on the eigenvectors:

$$\{|\tilde{1}\rangle = e^{-i\omega t}|1\rangle, \quad |\tilde{0}\rangle = |0\rangle, \quad |\tilde{-1}\rangle = |-1\rangle\}. \quad (4.1)$$

As expected, the Hamiltonian becomes stationary in the rotating frame:

$$\mathbf{H} = \omega_0(\tilde{\mathbf{P}}_1 - \tilde{\mathbf{P}}_{-1}) + \epsilon(\tilde{\mathbf{P}}_{1,0} + \tilde{\mathbf{P}}_{0,1}), \quad (4.2)$$

where new projection operators in the rotating frame have been defined: $\tilde{\mathbf{P}}_{i,j} \equiv |\tilde{i}\rangle\langle\tilde{j}|$ and $\tilde{\mathbf{P}}_i \equiv \tilde{\mathbf{P}}_{i,i}$ ($i, j = -1, 0, 1$).

The thermodynamic observables can be expressed as functions of the projections $\{\tilde{\mathbf{P}}_{i,j}\}$ and therefore they

also become stationary in steady state. This is easily seen for the “power operator,” given by

$$\frac{\partial \mathbf{H}_I}{\partial t} = -i\epsilon(\tilde{\mathbf{P}}_{1,0} - \tilde{\mathbf{P}}_{0,1}). \quad (4.3)$$

The observables corresponding to the heat currents, to be constructed in Sec. VII, share the same property.

V. QUANTUM MASTER EQUATIONS

Consider an arbitrary quantum system with a time-independent free Hamiltonian. Coupling this system to a much larger quantum system which is in thermal equilibrium, i.e., a “heat reservoir,” will induce the relaxation of the system to a stationary equilibrium state. The reduced equilibrium density matrix will take the form $\rho_{eq} = e^{-\beta \mathbf{H}} / \text{Tr}(e^{-\beta \mathbf{H}})$, with \mathbf{H} the effective time-independent Hamiltonian of the system. This scenario has been extensively studied in the literature of open quantum systems [10,14]. Some of the main results of these studies, which are relevant to the present study, are considered below.

It was found in numerous applications that Markovian equations, also known as “quantum master equations,” provide an excellent description of relaxation phenomena for systems with time-independent free Hamiltonians [6,8,10,15,16]. Furthermore, Markovian equations can be derived by explicitly carrying out the reduction from the Hamiltonian dynamics of the extended system, consisting of the system plus reservoir, to the internal dynamics of the system. The reduced dynamics is given by master equations provided the time scale of the bath fluctuations is much faster than that of the system’s relaxation. Such a separation of time scales is valid in the weak coupling limit and the singular bath limit.

The semigroup school [10,17,18] provides the basis for a generalized approach towards the description of non-Hamiltonian dynamics. In this approach the semigroup condition is axiomatically imposed on the evolution. This means that the evolution will be Markovian and keep the density matrix completely positive. This set of axioms guarantees that the non-Hamiltonian dynamics of the system can be realized by performing the reduction from a system plus reservoir Hamiltonian dynamics. Lindblad and Kossakowski and co-workers obtained the universal form of the generator for all the possible dynamical semigroup maps [17,18]. Thus the semigroup approach provides the most general form of the quantum master equation which, in the Heisenberg picture, is given by

$$\dot{\mathbf{X}} = i[\mathbf{H}, \mathbf{X}] + \frac{\partial \mathbf{X}}{\partial t} + \mathcal{L}_D(\mathbf{X}), \quad (5.1)$$

$$\mathcal{L}_D(\mathbf{X}) = \sum_{\alpha} \gamma_{\alpha} (\mathbf{V}_{\alpha}^{\dagger}[\mathbf{X}, \mathbf{V}_{\alpha}] + [\mathbf{V}_{\alpha}^{\dagger}, \mathbf{X}]\mathbf{V}_{\alpha}). \quad (5.2)$$

The operators \mathbf{V}_{α} , $\mathbf{V}_{\alpha}^{\dagger}$, \mathbf{H} , and \mathbf{X} are defined in the Hilbert space of the system. \mathbf{H} is the effective Hamiltonian of the system when coupled to the reservoir. It is usually a good approximation to substitute the free

Hamiltonian for \mathbf{H} , in the limit of weak coupling to the heat reservoir. Thus the first term on the right-hand side of Eq. (5.1) contains the Hamiltonian-unitary-reversible contribution to the dynamics. The operators \mathbf{V}_{α} and $\mathbf{V}_{\alpha}^{\dagger}$ are Hermitian conjugates, and, like \mathbf{H} in the theory of Hamiltonian dynamics, are not determined by the theory. The parameters $\{\gamma_{\alpha}\}$ are positive rate coefficients. The second term on the right-hand side of Eq. (5.1) contains the non-Hamiltonian (i.e., nonunitary) and irreversible contribution to the dynamics.

The description of the three-level system interacting with two heat reservoirs can be split into that of two effective two-level subsystems, each interacting with a single heat reservoir. For the relaxation of a two-level system with the free Hamiltonian

$$\mathbf{H} = \epsilon_g |g\rangle\langle g| + \epsilon_e |e\rangle\langle e|, \quad (5.3)$$

a reasonable choice for the operators $\{\mathbf{V}_{\alpha}\}$ in Eq. (5.2) are the Fermionic creation and annihilation operators: $\mathbf{P}_{e,g} \equiv |e\rangle\langle g|$, and $\mathbf{P}_{g,e} \equiv |g\rangle\langle e|$ ($\epsilon_g < \epsilon_e$). This choice leads to the following equation of motion:

$$\begin{aligned} \dot{\mathbf{X}} = & i[\mathbf{H}, \mathbf{X}] + \gamma_+ (2\langle e|\mathbf{X}|e\rangle \cdot \mathbf{P}_g - \{\mathbf{P}_g, \mathbf{X}\}) \\ & + \gamma_- (2\langle g|\mathbf{X}|g\rangle \cdot \mathbf{P}_e - \{\mathbf{P}_e, \mathbf{X}\}), \end{aligned} \quad (5.4)$$

where $\{\mathbf{A}, \mathbf{B}\}$ is the anticommutator: $\{\mathbf{A}, \mathbf{B}\} \equiv \mathbf{AB} + \mathbf{BA}$. The system asymptotically reaches thermal equilibrium if the rate coefficients comply with detailed balance:

$$\frac{\gamma_-}{\gamma_+} = e^{(\epsilon_e - \epsilon_g)/T}, \quad (5.5)$$

where T is the temperature of the heat reservoir.

Bloch equations [19] emerge when substituting the spin polarization components, \mathbf{S}_x , \mathbf{S}_y and \mathbf{S}_z , for \mathbf{X} in Eq. (5.4). Then $1/\tau_1 = 2(\gamma_- + \gamma_+)$ and $1/\tau_2 = (\gamma_- - \gamma_+)$, where the relaxation time constants τ_1 and τ_2 correspond to the population relaxation and dephasing, respectively. The choice in Eq. (5.5) indeed leads the system asymptotically to the correct equilibrium polarization: $\langle \mathbf{S}_x \rangle_{\infty} = \langle \mathbf{S}_y \rangle_{\infty} = 0$, $\langle \mathbf{S}_z \rangle_{\infty} = -\frac{1}{2} \tanh\left[\frac{\epsilon_e - \epsilon_g}{2T}\right]$. It should be noted that Bloch equations have been derived from the reduced dynamics of a two-level system in the limit of weak coupling to the heat reservoir [6,8]. That τ_2 is twice as large as τ_1 is characteristic of the case of nondiagonal coupling between the system and the heat reservoir. Diagonality in this context is defined with respect to the eigenstates of the free Hamiltonian. Diagonal coupling will add further dephasing, so that $1/\tau_2 = 1/(2\tau_1) + 1/\tau_2'$, where $1/\tau_2'$ is a pure dephasing term [6,20].

Detailed balance provides one constraint imposed on the two rate coefficients. Since the specific dependence of the rate coefficients on the field strength is important for the present study, a specific model for the heat reservoirs is adopted. A standard choice is that of reservoirs consisting of uncoupled normal modes. The coupling between the system and the reservoir is assumed linear in the coordinates of the normal modes. For this choice, explicit expressions for the rate coefficients can be derived in the limit of weak coupling with the reservoir [8]:

$$\gamma_+ = \mu(\Delta\epsilon)^3 n(\Delta\epsilon/T), \quad \gamma_- = \mu(\Delta\epsilon)^3 [n(\Delta\epsilon/T) + 1], \quad (5.6)$$

where $\Delta\epsilon \equiv \epsilon_e - \epsilon_g$ and

$$n(x) = \frac{1}{e^x - 1}. \quad (5.7)$$

μ is a constant parameter which determines the strength of the atom-reservoir interaction. For example, if the reservoir consists of a radiation field, μ is proportional to the square of the dipole matrix element corresponding to the relevant transition. Energy units such that $\Delta\epsilon \approx 1$ are used, so that the assumption of weak coupling to the reservoir implies that $\mu \ll 1$. The cubic term in Eq. (5.6) is due to the choice of coupling linear in $\sqrt{\Delta\epsilon}$ and a density of states of the reservoir quadratic in $\Delta\epsilon$. These assumptions correspond to heat reservoirs consisting of radiation field or of acoustic phonons [8]. The last term in Eq. (5.6) is just the thermal population of the reservoir oscillator which is in resonance with the corresponding atomic transition. The above expressions for the rate coefficients are also consistent with detailed balance.

VI. THE THERMODYNAMIC INCONSISTENCY OF A FIELD-INDEPENDENT DISSIPATION

The simplest assumption concerning dissipation in the continuous heat engine model would be that the dissipation superoperators, \mathcal{L}_D^c and \mathcal{L}_D^h , are not affected by the presence of the external time-dependent field. In such a case \mathcal{L}_D^h is constructed to relax the unperturbed two-level subsystem $\{|-1\rangle, |1\rangle\}$ to thermal equilibrium at temperature T_h , and \mathcal{L}_D^c to relax the unperturbed two-level subsystem $\{|-1\rangle, |0\rangle\}$ to thermal equilibrium at temperature T_c . Lamb's semiclassical model for a three-level laser is based upon such an assumption of field-independent dissipation [8,21]. The dissipation superoperators then assume the form of Eq. (5.4):

$$\begin{aligned} \mathcal{L}_D^h(\mathbf{X}) = & \gamma_+^h (2\langle 1|\mathbf{X}|1\rangle \cdot \mathbf{P}_{-1} - \{\mathbf{P}_{-1}, \mathbf{X}\}) \\ & + \gamma_-^h (2\langle -1|\mathbf{X}|-1\rangle \cdot \mathbf{P}_1 - \{\mathbf{P}_1, \mathbf{X}\}), \end{aligned} \quad (6.1)$$

$$\begin{aligned} \mathcal{L}_D^c(\mathbf{X}) = & \gamma_+^c (2\langle 0|\mathbf{X}|0\rangle \cdot \mathbf{P}_{-1} - \{\mathbf{P}_{-1}, \mathbf{X}\}) \\ & + \gamma_-^c (2\langle -1|\mathbf{X}|-1\rangle \cdot \mathbf{P}_0 - \{\mathbf{P}_0, \mathbf{X}\}). \end{aligned} \quad (6.2)$$

The ratios of the rate coefficients comply with detailed balance:

$$\frac{\gamma_-^h}{\gamma_+^h} = e^{2\omega_0/T_h}, \quad \frac{\gamma_-^c}{\gamma_+^c} = e^{\omega_0/T_c}. \quad (6.3)$$

By construction the field parameters ϵ and ω are absent from the dissipation terms.

Implementing Eqs. (6.1) and (6.2) into Eq. (2.3) and solving for steady state, the following expressions are obtained for heat currents:

$$\dot{Q}_h = 4\omega_0(\gamma_+^h \tilde{P}_{-1} - \gamma_-^h \tilde{P}_1) - \epsilon\gamma_-^h(\tilde{P}_{0,1} + \tilde{P}_{1,0}), \quad (6.4)$$

$$\dot{Q}_c = 2\omega_0(\gamma_+^c \tilde{P}_{-1} - \gamma_-^c \tilde{P}_0) - \epsilon\gamma_-^c(\tilde{P}_{0,1} + \tilde{P}_{1,0}) \quad (6.5)$$

$$(\tilde{P}_{i,j} \equiv \langle \tilde{\mathbf{P}}_{i,j} \rangle, \tilde{P}_i \equiv \langle \tilde{\mathbf{P}}_{i,i} \rangle).$$

The expected population relaxation induced by heat exchange between the reservoirs and the working medium is described by the first terms on the right-hand side of Eqs. (6.4) and (6.5). The second terms, involving coherences, are nonphysical since they lead to the following inconsistency with thermodynamics: the steady-state efficiency can exceed the Carnot efficiency, and may even exceed 1, in violation of the second law of thermodynamics. A possible fix by arbitrarily neglecting the dephasing terms in Eqs. (6.4) and (6.5) leads to a violation of the first law of thermodynamics [Eq. (3.4)].

The source of this inconsistency can be traced back to the fact that the structure of the Hamiltonian of working medium is built into the dissipation superoperator, via the detailed balance relations and the creation and annihilation operators. In the field-independent approach, the dissipation superoperator "knows" how to relax a field-free system, while the real Hamiltonian contains an additional term corresponding to the interaction with the field. The nonphysical terms in Eqs. (6.4) and (6.5) emerge from operating with the field-independent dissipation superoperator on this term.

It is interesting to note that, under the assumptions of the present section, the power in steady state does not have a maximum as a function of the amplitude ϵ . Thus according to Lamb's analysis the power monotonically increases from zero as ϵ increases until it reaches saturation. The rise in power as ϵ increases is due to the increase of the probability for induced emission, which is quadratic in ϵ . The power saturates since the degree of population inversion asymptotically decreases as $1/\epsilon^2$ [8].

VII. A FIELD-DEPENDENT LIOUVILLIAN

A field-dependent approach to dissipation, which is consistent with thermodynamics, is provided in the present section. Basing the relaxation equations on the instantaneous full Hamiltonian rather than the field-free Hamiltonian leads to a consistent theory. One way of constructing such a field-dependent quantum master equation would be to use Eq. (5.4) with the detailed balance relations corresponding to the energy levels of the instantaneous Hamiltonian, and the creation and annihilation operators based upon the eigenstates of the instantaneous Hamiltonian.

This approach is by no means general. Its major advantages are (a) it will prove consistent with thermodynamics and (b) it will naturally yield itself for interpretation in terms of the standard theory.

The major limitations of this approach follow.

(a) The dynamics is assumed to be governed by an equation of the form of Eq. (5.4). The latter was originally derived for a time-independent free Hamiltonian. Its application in the presence of the field, with the instantaneous Hamiltonian substituting the constant Hamiltonian of the original derivation, involves an assumption concerning the separation of time scales. Three time scales are involved here: that of the decay of the reservoir's fluctuations ($\approx \tau_R$), that of the time-dependent field ($\approx \tau_F \approx 2\pi/\omega$), and that of the system's relaxation ($\approx \tau_S$). In the derivation of Eq. (5.4) for a system with a time-independent Hamiltonian, it is assumed that $\tau_R \ll \tau_S$ (cf. Sec. V). If $\tau_R \ll \tau_F$ the derivation of Eq. (5.4) is still valid, with the instantaneous Hamiltonian in place of the time-independent Hamiltonian in each "time grain" [6,22]. Thus the field is assumed to be slowly varying compared with the fluctuations of the heat reservoirs.

(b) The above approach considers only nondiagonal coupling to the heat reservoirs. Furthermore, the contribution of nondiagonal coupling, represented by μ , does not depend on the field. Yet, in the present context diagonality is defined in terms of the eigenstates of the instantaneous Hamiltonian. Thus a coupling considered nondiagonal at one field intensity might turn diagonal at another intensity. Incorporating this mechanism into the dynamics requires the derivation of the quantum master equations in the weak coupling limit. This requires treating the coupling to the heat reservoirs in terms of a full three-level system rather than two effective two-level subsystems (cf. the Appendix).

The field-dependent approach for the description of the amplifier's dynamics is now presented. Diagonalizing the full Hamiltonian, $\mathbf{H} = \mathbf{H}_0 + \mathbf{H}_I$, at a given instant in time, yields the following instantaneous eigenvalues:

$$E_{-1} = -\omega_0, \quad (7.1)$$

$$E_0 = \frac{\omega_0}{2} - \sqrt{\left(\frac{\omega_0}{2}\right)^2 + \epsilon^2}, \quad (7.2)$$

$$E_1 = \frac{\omega_0}{2} + \sqrt{\left(\frac{\omega_0}{2}\right)^2 + \epsilon^2}. \quad (7.3)$$

The correlation diagram of the levels is shown in Fig. 3. Note that although the Hamiltonian is explicitly time dependent, its instantaneous eigenvalues are stationary. However, they do depend on the field amplitude ϵ so that the energy difference between the levels coupled by the field increases as $|\epsilon|$ increases. A unitary "rotation" transformation relates the new eigenstates to the old ones:

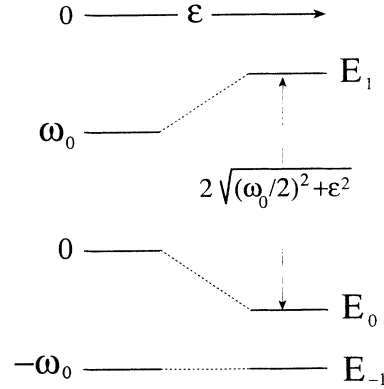


FIG. 3. A correlation diagram showing the instantaneous energy levels of the field-dependent Hamiltonian. These energy levels depend on the field amplitude ϵ . The horizontal arrow at the top indicates the direction of increasing ϵ .

$$\begin{aligned} \begin{pmatrix} |E_1\rangle \\ |E_0\rangle \\ |E_{-1}\rangle \end{pmatrix} &= \begin{pmatrix} \cos(\theta/2)e^{-i\omega t} & \sin(\theta/2) & 0 \\ -\sin(\theta/2)e^{-i\omega t} & \cos(\theta/2) & 0 \\ 0 & 0 & 1 \end{pmatrix} \\ &\times \begin{pmatrix} |1\rangle \\ |0\rangle \\ |-1\rangle \end{pmatrix} \\ &= \begin{pmatrix} \cos(\theta/2) & \sin(\theta/2) & 0 \\ -\sin(\theta/2) & \cos(\theta/2) & 0 \\ 0 & 0 & 1 \end{pmatrix} \\ &\times \begin{pmatrix} |\tilde{1}\rangle \\ |\tilde{0}\rangle \\ |-\tilde{1}\rangle \end{pmatrix}, \quad (7.4) \end{aligned}$$

where the angle θ is given by $\tan(\theta) = 2\epsilon/\omega_0$. These eigenvectors are explicitly time dependent. They become stationary in a reference frame rotating at the frequency ω .

The transformation from the representation diagonal in \mathbf{H}_0 to the representation diagonal in \mathbf{H} may be interpreted in geometrical terms (cf. Fig. 4). Since only the two upper states are coupled by the field, an analogy to a spin-1/2 system interacting with a magnetic field can be used. The field-free Hamiltonian of this fictitious two-level subsystem is $\omega_0\mathbf{P}_1$, analogous to that of a spin-1/2 system in a constant magnetic field. Consider a stationary Cartesian coordinate system, (x, y, z) , so that the constant magnetic field lies along the z axis. The representation diagonal in $\omega_0\mathbf{P}_1$ is equivalent to that diagonal in \mathbf{S}_z . The basis functions of this representation are $|0\rangle, |1\rangle$.

The full Hamiltonian of the fictitious two-level subsystem is $\omega_0\mathbf{P}_1 + \mathbf{H}_I$, which is analogous to a spin-1/2 system interacting with a rotating magnetic field. This field has constant component along the z axis, of magnitude ω_0/γ , and a component of magnitude $2\epsilon/\gamma$, rotating with the frequency ω in the (x, y) plane (γ is the gyro-magnetic ratio) [6,15]. The angle between this fictitious magnetic field and the z axis is θ . The angle between the component of the field in the (x, y) plane and the x axis,

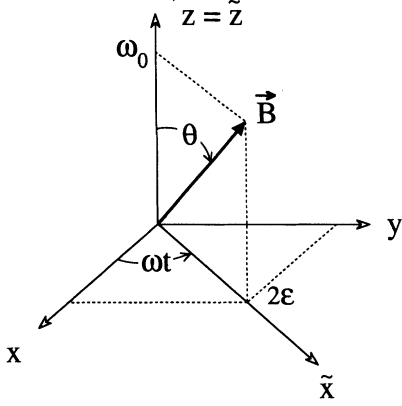


FIG. 4. The geometrical interpretation in terms of a fictitious two-level system, interacting with a rotating magnetic field. The coordinates system (x, y, z) is stationary, while the coordinate system $(\tilde{x}, \tilde{y}, \tilde{z})$ rotates with the frequency ω around the z axis, so that the \tilde{x} axis coincides with the (x, y) component of the fictitious magnetic field.

at a given instant, is ωt . The representation diagonal in the instantaneous full Hamiltonian is equivalent to that diagonal in the spin component along the instantaneous direction of the field. The instantaneous basis of this representation is $|E_0\rangle, |E_1\rangle$.

The transformation from the representation diagonal in S_z to that diagonal in the spin component along the direction of the rotating field therefore consists of two rotations: one, of angle ωt around the z axis, and the other, of angle θ in the plane defined by the rotating field and the z axis. This indeed is the transformation in Eqs. (7.4). The instantaneous direction of the rotating field is denoted as “the relaxation axis” for later use.

Next, projection operators in terms of the instantaneous eigenvectors of the Hamiltonian are defined:

$$\Pi_{i,j} = |\mathbf{E}_i\rangle\langle\mathbf{E}_j|, \quad \Pi_{i,i} \equiv \Pi_i, \quad \{i, j = -1, 0, 1\}. \quad (7.5)$$

The projection operators $\Pi_{1,-1}$ and $\Pi_{-1,1}$ are the instantaneous creation and annihilation operators corresponding to the coupling with the hot reservoir. The projection operators $\Pi_{0,-1}$ and $\Pi_{-1,0}$ are the instantaneous creation and annihilation operators corresponding to the coupling with the cold reservoir. These projections are implemented into a quantum master equation of the form of Eq. (5.4). The dissipation superoperators in the Heisenberg picture then become

$$\begin{aligned} \mathcal{L}_D^h(\mathbf{X}) &= \gamma_+^h (2\langle E_1|\mathbf{X}|E_1\rangle \cdot \Pi_{-1} - \{\Pi_{-1}, \mathbf{X}\}) \\ &+ \gamma_-^h (2\langle E_{-1}|\mathbf{X}|E_{-1}\rangle \cdot \Pi_1 - \{\Pi_1, \mathbf{X}\}), \end{aligned} \quad (7.6)$$

$$\begin{aligned} \mathcal{L}_D^c(\mathbf{X}) &= \gamma_+^c (2\langle E_0|\mathbf{X}|E_0\rangle \cdot \Pi_{-1} - \{\Pi_{-1}, \mathbf{X}\}) \\ &+ \gamma_-^c (2\langle E_{-1}|\mathbf{X}|E_{-1}\rangle \cdot \Pi_0 - \{\Pi_0, \mathbf{X}\}). \end{aligned} \quad (7.7)$$

The ratios of the rate coefficients now comply with instantaneous detailed balance relations, corresponding to the field-shifted energy levels:

$$\frac{\gamma_-^h}{\gamma_+^h} = e^{(E_1 - E_{-1})/T_h}, \quad \frac{\gamma_-^c}{\gamma_+^c} = e^{(E_0 - E_{-1})/T_c}. \quad (7.8)$$

For weak dipolelike interaction with a heat reservoir consisting of uncoupled normal modes the rate coefficients become [Eq. (5.6)]

$$\begin{aligned} \gamma_+^h &= \mu(E_1 - E_{-1})^3 n[\beta_h(E_1 - E_{-1})], \\ \gamma_-^h &= \mu(E_1 - E_{-1})^3 \{n[\beta_h(E_1 - E_{-1})] + 1\}, \end{aligned} \quad (7.9)$$

$$\begin{aligned} \gamma_+^c &= \mu(E_0 - E_{-1})^3 n[\beta_c(E_0 - E_{-1})], \\ \gamma_-^c &= \mu(E_0 - E_{-1})^3 \{n[\beta_c(E_0 - E_{-1})] + 1\}. \end{aligned} \quad (7.10)$$

The same value of the working medium-reservoir coupling constant μ is chosen for both reservoirs.

The new dissipation superoperators explicitly depend upon the field parameters ϵ and ω . The instantaneous creation and annihilation operators are explicitly time dependent, while the rate coefficients are time independent. This is opposite to the quantum spin and harmonic engine models, where the creation and annihilation operators are stationary and the rate coefficients are explicitly time dependent [3,4].

By substituting \mathbf{H} for \mathbf{X} in Eq. (2.3), and using the new dissipation superoperators [Eqs. (7.6) and (7.7)], the following expressions for the power and heat currents in terms of the new set of instantaneous projectors are found:

$$\mathcal{P} = 2\epsilon\omega \text{Im}(\Pi_{1,0}), \quad (7.11)$$

$$\dot{Q}_h = (E_1 - E_{-1})(2\gamma_+^h \Pi_{-1} - 2\gamma_-^h \Pi_1), \quad (7.12)$$

$$\dot{Q}_c = -(E_1 - E_0)(2\gamma_-^c \Pi_0 - 2\gamma_+^c \Pi_{-1}), \quad (7.13)$$

where $\Pi_{i,j} \equiv \langle \Pi_{i,j} \rangle$, $\Pi_i \equiv \langle \Pi_i \rangle$. Note that the power is still proportional to the imaginary part of the coherence, now defined in terms of the representation diagonal in the instantaneous Hamiltonian. This is due to the fact that $\text{Im}(\Pi_{1,0})$ is analogous to the spin component along the rotating y axis, which is invariant under the rotation by θ around the rotating y axis. The heat currents correspond to population transfer between the instantaneous energy levels, and no longer contain artificial terms involving coherence. The reason for this is obvious: the new dissipation superoperators are designed to relax the total Hamiltonian \mathbf{H} , rather than \mathbf{H}_0 .

If the operators Π_1 , Π_0 , $\Pi_{1,0}$, and $\Pi_{0,1}$ are substituted for \mathbf{X} in Eq. (2.3), and the dissipation superoperators from Eqs. (7.6) and (7.7) are used, the following set of coupled equations of motion for the working medium observables is obtained:

$$\dot{\Pi}_{1,0} = -(\Gamma_- + i\widetilde{\Delta\omega})\Pi_{1,0} - i\tilde{\epsilon}\Pi_1 + i\tilde{\epsilon}\Pi_0, \quad (7.14)$$

$$\dot{\Pi}_{0,1} = -(\Gamma_- - i\widetilde{\Delta\omega})\Pi_{0,1} + i\tilde{\epsilon}\Pi_1 - i\tilde{\epsilon}\Pi_0, \quad (7.15)$$

$$\begin{aligned} \dot{\Pi}_1 &= -i\tilde{\epsilon}\Pi_{1,0} + i\tilde{\epsilon}\Pi_{0,1} - 2(\gamma_+^h + \gamma_-^h)\Pi_1 \\ &\quad - 2\gamma_+^h\Pi_0 + 2\gamma_+^h, \end{aligned} \quad (7.16)$$

$$\begin{aligned} \dot{\Pi}_0 &= i\tilde{\epsilon}\Pi_{1,0} - i\tilde{\epsilon}\Pi_{0,1} \\ &\quad - 2\gamma_+^c\Pi_1 - 2(\gamma_+^c + \gamma_-^c)\Pi_0 + 2\gamma_+^c, \end{aligned} \quad (7.17)$$

where:

$$\begin{pmatrix} 2\tilde{\epsilon} \\ \widetilde{\Delta\omega} \end{pmatrix} = \begin{pmatrix} \cos(\theta) & -\sin(\theta) \\ \sin(\theta) & \cos(\theta) \end{pmatrix} \begin{pmatrix} 2\epsilon \\ \Delta\omega \end{pmatrix}, \quad (7.18)$$

$$\Delta\omega = \omega_0 - \omega, \quad (7.19)$$

$$\Gamma_- = \gamma_-^h + \gamma_-^c. \quad (7.20)$$

Equations (7.14)–(7.17) have a form similar to the equations obtained from Lamb’s semiclassical theory for lasers [8]. However, the relaxation in Lamb’s theory is modeled by using the field-independent approach of Sec. VI. This crucial difference is made apparent by the following facts.

(a) The populations and coherence in Eqs. (7.14)–(7.17) are given in terms of the representation diagonal in \mathbf{H} , while in Lamb’s theory they are given in terms of the representation diagonal in \mathbf{H}_0 .

(b) Instead of the usual detuning, $\Delta\omega$, and amplitude, ϵ , as in Lamb’s theory, new, “rotated,” detuning $\widetilde{\Delta\omega}$ and amplitude $\tilde{\epsilon}$ are defined. An interpretation can be based on the geometrical picture in terms of a spin- $\frac{1}{2}$ system interacting with a rotating magnetic field. (cf. Figs. 4,5.) Consider the reference frame, $(\tilde{x}, \tilde{y}, \tilde{z})$, rotating at

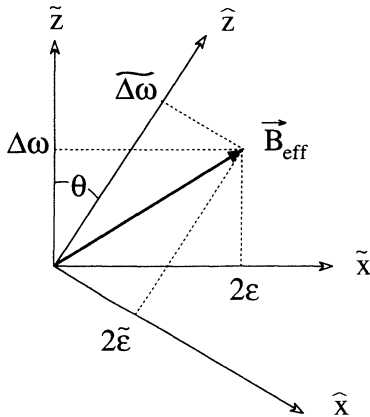


FIG. 5. The rotated detuning and amplitude. \tilde{z} is the relaxation axis in Lamb’s model. The detuning, i.e., the field component parallel to the relaxation axis, is $\Delta\omega$, and the effective component of the field, i.e., the field component perpendicular to the relaxation axis, is 2ϵ . \tilde{z} is the relaxation axis in the field-dependent model, so that $\widetilde{\Delta\omega}$ and $2\tilde{\epsilon}$ are the “rotated” detuning and field amplitude, respectively.

a frequency ω around the original z axis, with the \tilde{x} axis coinciding with the rotating component of the magnetic field in the (x, y) plane. An observer moving with this rotating frame sees a stationary field in the (\tilde{x}, \tilde{z}) plane, whose \tilde{x} and \tilde{z} components are 2ϵ and $\Delta\omega$, respectively. The heat reservoirs induce relaxation which gradually diminishes the polarization perpendicular to the relaxation axis while establishing a “stationary” polarization along the relaxation axis. The role of the relaxation is to restore the polarization (i.e., the population inversion) destroyed by the field when inducing emission. It can only do so along the relaxation axis. Thus only the field component perpendicular to the relaxation axis will be effective in continuous lasing. The other component, parallel to the relaxation axis, constitutes the detuning. Since the relaxation axis in Lamb’s model lies along the $z \equiv \tilde{z}$ axis, the effective field component is 2ϵ , while the detuning is $\Delta\omega$. However, in the present model, the relaxation axis is rotated in the (\tilde{x}, \tilde{z}) plane by an angle θ with respect to the z axis. Thus $2\tilde{\epsilon}$ is the effective field component, while $\widetilde{\Delta\omega}$ is the detuning.

(c) Although still stationary, the rate coefficients now explicitly depend on ϵ . The rate coefficients in Lamb’s theory are field independent.

VIII. THE STEADY-STATE SOLUTION

Explicit expressions for stationary thermodynamical quantities are obtained by solving Eqs. (7.14)–(7.17) for steady state. For the power and heat currents Eqs. (7.11)–(7.13) one finds

$$\dot{Q}_h^{ss} = (E_1 - E_{-1})W \frac{\Pi_1^0 - \Pi_0^0}{1 + W/\Gamma}, \quad (8.1)$$

$$\dot{Q}_c^{ss} = -(E_0 - E_{-1})W \frac{\Pi_1^0 - \Pi_0^0}{1 + W/\Gamma}, \quad (8.2)$$

$$P^{ss} = -(E_1 - E_0)W \frac{\Pi_1^0 - \Pi_0^0}{1 + W/\Gamma}. \quad (8.3)$$

Substituting these results into Eq. (3.6), the following expression is obtained for the steady-state efficiency:

$$\eta = \frac{E_1 - E_0}{E_1 - E_{-1}}. \quad (8.4)$$

The right-hand side in Eqs. (8.1)–(8.3) is factorizable into three contributions. Each of these contributions is separately analyzed.

A. The energy difference

The first term in Eqs. (8.1)–(8.3) is the energy difference between the two field-shifted levels. Obviously, the energy flow through each transition is proportional to the energy gain, or loss, per transition. The expressions for

the heat currents and power in steady state are identical except for the first term. Thus the steady-state efficiency, which is given by their ratio, reduces to the ratio of the energy differences associated with the work and hot reservoirs [Eq. (8.4)]. Note that the energy differences depend on the field amplitude ϵ , so that the energy differences associated with the hot and work reservoirs increases, while that associated with the cold reservoir decreases, as the field amplitude increases (cf. Fig. 3). The ϵ dependence of this term is crucial for obtaining consistency with thermodynamics, as will be shown below. However, the ϵ dependence of this term is relatively weak compared with that of the other two terms, and therefore does not play a dominant role when ϵ is used as a control.

B. The transition probability

W is the probability per unit time for a field-induced transition between the levels $|E_0\rangle$ and $|E_1\rangle$. Since the energy of the system is constant in steady state, a transition between $|E_1\rangle$ and $|E_0\rangle$ is accompanied by transitions between $|E_0\rangle$ and $|E_{-1}\rangle$ and between $|E_{-1}\rangle$ and $|E_1\rangle$. Thus W is the probability per unit time for each of the transitions.

W is explicitly given by

$$W = \frac{2\tilde{\epsilon}^2 \Gamma_-}{\Gamma_-^2 + \widetilde{\Delta\omega}^2}. \quad (8.5)$$

Equation (8.5) is similar in form to the expression obtained for W in Lamb's model:

$$W_{\text{Lamb}} = \frac{2\epsilon^2 \Gamma_-}{\Gamma_-^2 + \Delta\omega^2}. \quad (8.6)$$

However, W and W_{Lamb} differ in two respects.

(a) The rotated $\tilde{\epsilon}$ and $\widetilde{\Delta\omega}$ in Eq. (8.5) replace ϵ and $\Delta\omega$ from Lamb's model. This is because the relaxation axis in the present study is rotated by an angle θ with respect to the relaxation axis in Lamb's model.

(b) In Lamb's model Γ_- is independent of the field parameters in accordance with the assumption of field-independent dissipation. However, Γ_- is explicitly ϵ dependent in the present model [cf. Eqs. (7.2) and (7.3), (7.9) and (7.10)].

Comparing the behavior of W and W_{Lamb} as a function of the amplitude ϵ and the detuning, $\Delta\omega$, the following observations are made

(a) W_{Lamb} is a parabolic function of ϵ [cf. Eq. (8.6)]. The ϵ dependence of W is more complex. For small ϵ it, too, is parabolic in ϵ . Yet, as ϵ becomes larger, W reaches a maximum and starts decreasing as a function of ϵ (cf. Fig. 6). Two factors combine to induce this effect:

(1) As ϵ increases, its relative contribution to the effective component of the field, $\tilde{\epsilon}$, diminishes, while its contribution to the effective detuning, $\widetilde{\Delta\omega}$, increases.

(2) Γ_- is monotonically increasing in ϵ , so that the denominator in Eq. (8.5) also increases with ϵ . The de-

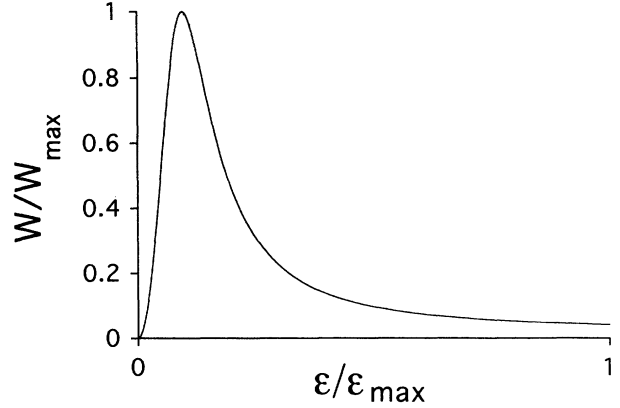


FIG. 6. The normalized probability per unit time for a field-induced transition, W/W_{max} , as a function of the normalized field amplitude, $\epsilon/\epsilon_{\text{max}}$. The parameters used are $\omega_0 = 1.00$, $T_c = 0.05$, $T_h = 0.50$, $\mu = 0.005$, and $\Delta\omega = 0.00$.

pendence of W on Γ_- should be noted. For small Γ_- , W increases linearly as Γ_- increases. In this region, a bigger Γ_- implies more efficient pumping, cooling, and lasing. Yet, as Γ_- become bigger, the Γ_-^2 term in the denominator in the right-hand side of Eq. (8.5) becomes dominant and diminishes W . This effect is due to the dephasing of $\Pi_{1,0}$, which weakens the power output mechanism [cf. Eq. (7.11)]. Since population relaxation and dephasing are inseparable and have counter effects on W , there is a trade-off between them which will play a role in determining the maximum power when ϵ is used as a control.

(b) W as a function of the field frequency ω is plotted in Fig. 7 for different values of the amplitude ϵ . W has a sharp peak, and the value of ω at the maximum of this peak is given by

$$\omega^* = \omega_0 + \frac{\Gamma_-^2 + (2\epsilon)^2}{\omega_0}. \quad (8.7)$$

Thus the optimal operation frequency of the amplifier

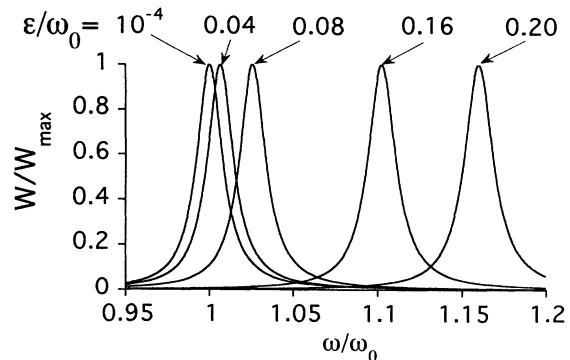


FIG. 7. W (normalized), as a function of the normalized frequency, in the resonance domain. The numbers associated with each peak correspond to the value of normalized field amplitude, ϵ/ω_0 . The parameters of the calculation are $\omega_0 = 1.000$, $T_c = 0.050$, $T_h = 0.500$, $\mu = 0.001$.

is obtained above the “standard resonance” (i.e., at $\omega > \omega_0$). The deviation from “standard resonance” is significant for intense fields (cf. Fig. 7) since $\Gamma_-/\omega_0 \ll 1$ for the master equation to be valid (cf. Sec. V). The maximization of W with respect to the frequency ω , for a given field amplitude ϵ , leads to the following maximal value of W :

$$W^* = \frac{2\epsilon^2(\Gamma_-^2 + \omega_0^2 + 4\epsilon^2)}{\omega_0^2\Gamma_-}. \quad (8.8)$$

Unlike W , W^* is a monotonically increasing function of ϵ (cf. Fig. 8), because the frequency ω^* follows the shift of W towards higher frequencies (cf. Fig. 7). Finally, the off-resonance behavior is shown in Fig. 9. W reduces to zero as ω approaches zero, as expected. It should be noted that this is not the case for W_{Lamb} [cf. Eq. (8.6)]. As $|\omega|$ becomes very large, W asymptotically approaches the following finite value:

$$W_\infty = \frac{\Gamma_-}{2} \tan^2(\theta). \quad (8.9)$$

It should be noted that W_{Lamb} asymptotically reduces to zero as the $|\omega|$ increases. As expected, the difference between the two approaches becomes significant only when the field is intense.

C. The population inversion

The last term in the right-hand side of Eqs. (8.1)–(8.3) corresponds to the steady-state population difference between the two levels coupled to the field, namely,

$$\Pi_1^{ss} - \Pi_0^{ss} = \frac{\Pi_1^0 - \Pi_0^0}{1 + W/\Gamma}. \quad (8.10)$$

The terms Π_0^0 and Π_1^0 can be understood as representing the stationary population occupancies of a fictitious three-level system, coupled to the same heat reservoirs.

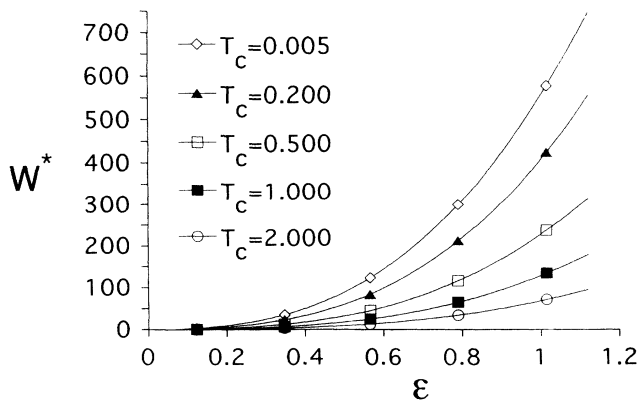


FIG. 8. W^* , i.e., W maximized with respect to the field frequency, as a function of the field amplitude for various temperatures. The parameters of the calculation are $T_c/T_h = 0.100$, $\mu = 0.001$.

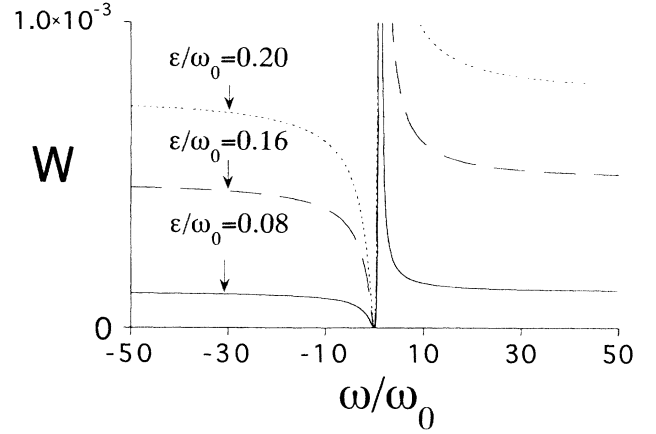


FIG. 9. W as a function of the normalized frequency, ω/ω_0 , in the off-resonance domain, for different values of field amplitude, ϵ . Notice that W asymptotically decays to a finite value, rather than zero, as $|\omega/\omega_0| \gg 1$.

The energy levels of this system in the absence of the external field are E_{-1} , E_0 , and E_1 . The population occupancies are explicitly given by

$$\Pi_0^0 = \frac{\gamma_-^h \gamma_+^c}{\gamma_-^h \gamma_-^c + \gamma_-^h \gamma_+^c + \gamma_+^h \gamma_-^c}, \quad (8.11)$$

$$\Pi_1^0 = \frac{\gamma_+^h \gamma_-^c}{\gamma_-^h \gamma_-^c + \gamma_-^h \gamma_+^c + \gamma_+^h \gamma_-^c}. \quad (8.12)$$

Finally Γ in Eq. (8.10) is given by

$$\Gamma = \frac{2(\gamma_-^h \gamma_-^c + \gamma_-^h \gamma_+^c + \gamma_+^h \gamma_-^c)}{\Gamma_- + 2(\gamma_+^h + \gamma_-^c)}. \quad (8.13)$$

Note that Γ has the dimension of a rate coefficient.

Obviously, the amplifier has to amplify, meaning a net production of power which is defined by $\mathcal{P} \leq 0$. This can be obtained under the condition of population inversion, $\Pi_1^{ss} \geq \Pi_0^{ss}$ [cf. Eq. (8.3)]. Population inversion then requires that $\Pi_1^0 \geq \Pi_0^0$ [cf. Eq. (8.10)]. From Eqs. (8.11) and (8.12) one finds that $\Pi_1^0 \geq \Pi_0^0$ when

$$\frac{E_0 - E_{-1}}{E_1 - E_{-1}} \geq \frac{T_c}{T_h}. \quad (8.14)$$

Equation (8.14) therefore sets an upper bound on $|\epsilon|$ [cf. Eqs. (7.1)–(7.3)]:

$$|\epsilon| \leq \epsilon_{\text{max}} \equiv \omega_0 \frac{\sqrt{2(1 + \alpha^2) - 5\alpha}}{1 + \alpha}, \quad (8.15)$$

where $\alpha \equiv T_c/T_h$. For $\epsilon > \epsilon_{\text{max}}$ the device starts consuming power from the field and ceases to operate as an engine. Since the power is symmetric with respect to a change in the sign of ϵ [i.e., $\mathcal{P}(\epsilon) = \mathcal{P}(-\epsilon)$, cf. Eq. (8.3)], the field amplitude ϵ can be chosen non-negative, without loss of generality. Also note that T_h must be at least

twice as large as T_c if positive power production is to occur:

$$\frac{T_c}{T_h} < \frac{1}{2}. \quad (8.16)$$

Analyzing the numerator in Eq. (8.10), one finds that as ϵ increases, so does the energy difference $E_1 - E_{-1}$, while $E_0 - E_{-1}$ decreases. Thus stationary population in the level $|E_1\rangle$ (Π_1^0) reduces, while that in the level $|E_0\rangle$ (Π_0^0) increases (cf. Fig. 10). This amounts to a decrease in the numerator of Eq. (8.10) as ϵ increases, up to a point ($\epsilon = \epsilon_{\max}$) where it becomes zero. It should be noted that in Lamb's model, the populations Π_0^0 and Π_1^0 correspond to the unperturbed three-level atom and therefore do not depend on ϵ .

The power has a maximum as a function of ϵ since it is zero for both $\epsilon = 0$ and $\epsilon = \epsilon_{\max}$. This behavior is fundamentally different than that obtained from Lamb's model, where the power reaches saturation as the field amplitude increases. This allows a finite-time thermodynamic analysis of the performance of the amplifier, with the power as the target function and ϵ as the control (cf. Sec. IX).

The numerator in Eq. (8.10) stands for the "thermodynamic" population inversion in the absence of field-induced transitions, the denominator represents the "kinetic" effect on the steady-state population inversion. Field-induced transitions diminish the population inversion. Simultaneously, the population inversion is constantly restored by the relaxation processes. The steady-state population inversion is the result of trade-off between the two forces. Indeed, as the probability per second for a field-induced transition, W , increases the steady-state population inversion decreases [cf. Eq. (8.10)]. The coefficient Γ represents an effective rate coefficient characterizing the restoring "relaxation forces." As Γ increases, the steady-state population inversion increases. It should be noted that Γ decreases as ϵ increases. This represents the kinetical effect complementary to the thermodynamic effect in the numerator.

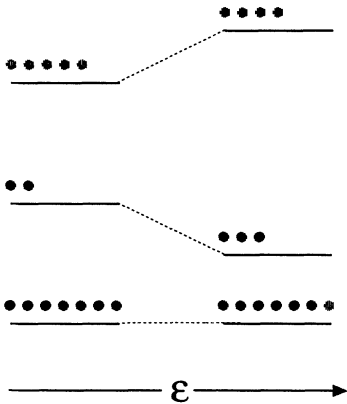


FIG. 10. A schematic view of the change in the population inversion $\Pi_1^0 - \Pi_0^0$ as a function of the field amplitude ϵ . Note that $\Pi_1^0 - \Pi_0^0$ decreases as ϵ increases. It eventually reduces to zero as ϵ reaches ϵ_{\max} . The arrow at the bottom indicates the direction of increasing ϵ .

The steady-state efficiency [Eq. (8.4)] has the following important properties

(a) The efficiency is bounded from above by the Carnot efficiency:

$$\eta \leq 1 - \frac{T_c}{T_h}. \quad (8.17)$$

This is an immediate consequence of Eq. (8.14). The efficiency reaches the Carnot efficiency [equality in Eq. (8.14)] only in the reversible limit, when the power is vanishingly small. Note that this important consistency with thermodynamics does not depend on the specific model used for the reservoir and is universal, depending only on the assumption of instantaneous detailed balance. From the microscopic point of view, the reversible limit corresponds to the population inversion threshold, in accordance with the work of Geusic, Schultz-du Bois, and Scovil, Levine and Kafri, and Ben-Shaul and Levine [7].

(b) The efficiency does not explicitly depend on the temperatures of the hot and cold reservoirs, and is a monotonically increasing function of ϵ . Its lower bound, $1/2$, is reached as ϵ approaches zero. The power and heat input then go to zero at the same rate. To reach the other limit where both the efficiency and the power are zero, one has to lift the constraint of constant energy difference between the subsequent unperturbed energy levels.

(c) The coherences $\Pi_{-1,0}$, $\Pi_{0,-1}$, $\Pi_{-1,1}$, and $\Pi_{1,-1}$ are zero in steady state. Thus the steady state of the reduced two-level subsystems that interact with the reservoirs is fully given by the populations (i.e., the diagonal density matrix elements). Since those are two-level systems, the population ratio uniquely define the corresponding internal temperatures:

$$T'_h \equiv \frac{E_1 - E_{-1}}{\ln(\Pi_{-1}^{ss}/\Pi_1^{ss})}, \quad T'_c \equiv \frac{E_0 - E_{-1}}{\ln(\Pi_{-1}^{ss}/\Pi_0^{ss})}, \quad (8.18)$$

where T'_c and T'_h are the internal temperatures of the $\{|E_{-1}\rangle, |E_0\rangle\}$ and $\{|E_{-1}\rangle, |E_1\rangle\}$ subsystems, respectively. If the engine produces power, while heat is being absorbed from the hot reservoir and ejected into the cold reservoir, the internal temperatures must be such that $T_c \leq T'_c$ and $T_h \geq T'_h$. Population inversion requires $\Pi_1^{ss} \geq \Pi_0^{ss}$, which, according to Eq. (8.18), may be put in the following form:

$$\eta \leq \eta_{\text{endo}} \equiv 1 - \frac{T'_c}{T'_h}. \quad (8.19)$$

η_{endo} , "the endoreversible efficiency," would have been the true efficiency if the only source of irreversibility is due to finite rate heat transfer between the working medium and the heat reservoirs. Equality in Eq. (8.19) is obtained only in the reversible limit, where $T_c = T'_c$ and $T_h = T'_h$. That the efficiency is lower than η_{endo} indicates that an additional source of irreversibility is involved. This extra source of irreversibility may be given two, complementary, interpretations.

(1) The first interpretation is based on an argument due to Levine and Kafri [7]. Population inversion in the

lasing transition leads to a negative internal temperature. The corresponding population ratio in steady state relates to this negative temperature, which is denoted by T'_p :

$$T'_p \equiv \frac{E_1 - E_0}{\ln(\Pi_0^{ss}/\Pi_1^{ss})} = \frac{E_1 - E_0}{(E_1 - E_{-1})/T'_h - (E_0 - E_{-1})/T'_c}. \quad (8.20)$$

Thus power production involves entropy production in the working medium, given by $\mathcal{P}/T'_p \geq 0$ (since both \mathcal{P} and T'_p are negative). The entropy of the working medium is constant in steady state. Thus the entropy production in the lasing transition adds to the entropy introduced into the working medium with the heat absorbed from the hot reservoir, and more heat must be dumped into the cold reservoir in order to maintain the entropy balance. Such an argument leads to the following efficiency:

$$\eta = \frac{1 - \frac{T'_c}{T'_h}}{1 - \frac{T'_c}{T'_p}}, \quad (8.21)$$

which is identical to the efficiency found in Eq. (8.4).

(2) Although consistent, the above interpretation is problematic in the following sense: the lasing two-level sub-system is not really in internal equilibrium, corresponding to a negative internal temperature, since the corresponding coherences, $\Pi_{1,0}$ and $\Pi_{0,1}$, are not zero in steady state. Furthermore, the whole mechanism of power production depends heavily upon the existence of these coherences [cf. Eq. (7.11)]. The following interpretation is therefore suggested: Finite power production requires finite coherence in steady state; the latter are constantly subject to thermal dephasing which destroys the coherence, unless some of the power is constantly invested to maintain it; the portion of power invested for this purpose is therefore constantly dissipated and ejected into the cold reservoir as heat. The power lost due to this source of irreversibility is given by the heat flux from hot reservoir multiplied by the difference between the endoreversible efficiency and the actual efficiency:

$$\Delta\mathcal{P}_{\text{lost}} \equiv [\eta_{\text{endo}} - \eta]\dot{Q}_h = T'_c \frac{\mathcal{P}}{T'_p}. \quad (8.22)$$

This lost energy is dumped as heat into the cold reservoir. Since this source of irreversibility lies in the coupling between the working medium and the work reservoir, it plays a role similar to that of classical friction, and may therefore be thought of as “quantum friction.”

IX. POWER OPTIMIZATION

The central theme of finite-time thermodynamics is the optimization of the performance of processes as a function of various controls. In the present work the steady-state power production of the amplifier, \mathcal{P} , is optimized with respect to three controls: (a) The rate of relaxation,

determined by μ , T_c , and T_h ; (b) the field’s frequency— ω ; and (c) the fields amplitude— ϵ .

It will be shown that the power has maxima as a function of the above controls. These maxima result from the following conflicts.

(a) Population relaxation is always accompanied by dephasing. As the relaxation rate increases, the pumping and cooling become faster (population relaxation), while the coupling with the field weakens (dephasing).

(b) As the interaction intensifies, the probability for field-induced transitions increases (at least for the low-field domain, cf. Sec. VIII), while the levels are shifted so that the pumping and cooling become slower.

(c) As ϵ becomes larger its contribution to the effective component of the field diminishes.

(d) As ϵ becomes larger, the energy released by the system per a single transition increases, while the net number of such transitions diminishes.

A. power optimization with respect to the coupling parameter (μ) and the heat reservoirs’ temperatures (T_c and T_h)

A direct observation of the interplay between population relaxation and dephasing is obtained when the coupling parameter μ is chosen as the control. μ determines the strength of coupling between the working medium and the heat reservoirs. It plays a role analogous to that of the heat conductivity in Newtonian heat engines.

The normalized power as a function of μ is plotted in Fig. 11, for constant frequency (ω) temperatures (T_c and T_h) and various values of the amplitude (ϵ).

The initial rise in power as μ increases is due to faster pumping and cooling, while the decrease in power as μ becomes larger is due to dephasing. The dephasing is more dominant for lower field amplitudes since the interaction with the field is then smaller to begin with, and therefore more sensitive to dephasing. Note that the validity of the whole model is restricted to $\mu/\omega_0 \ll 1$, which corresponds to the limit of weak coupling with the heat reservoirs. Thus the maximum in power as a function of

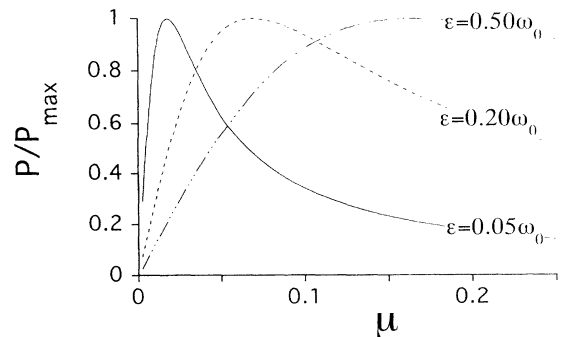


FIG. 11. The normalized power as a function of the system-bath coupling parameter μ , for various values of the field amplitude ϵ . The parameters of the calculation are $\omega_0 = 1.00$, $\Delta\omega = 0$, $T_c = 0.05$, and $T_h = 0.50$.

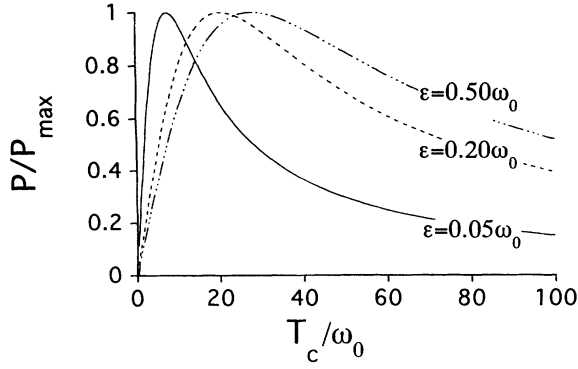


FIG. 12. The normalized power as a function of T_c for various values of the field amplitude ϵ . The parameters of the calculation are $T_c/T_h = 0.100$ and $\mu = 0.001$.

μ is only meaningful for low values of μ .

The same effect is viewed by looking at the power as a function of the temperatures of the heat reservoirs— T_c and T_h . In Fig. 12, the normalized power optimized with respect to ω is plotted as a function of T_c , for a given temperature ratio, and for various values of the field amplitude ϵ . As the temperatures increase, the relaxation becomes faster. For relatively small temperatures, this results in faster pumping and cooling, and therefore a rise in power. For larger temperatures dephasing takes over and the power decreases. Here too, the dephasing is more dominant for lower field amplitudes.

B. Power optimization with respect to the field frequency (ω)

The next control to be considered is the field frequency ω . The only term in the expression for the steady-state power that depends on ω is the transition probability W [Eq. (8.5)]. The power is also a monotonic function of W [Eq. (8.3)]. Thus optimizing the power with respect to ω is equivalent to the maximization of W with respect to ω . The optimal frequency, ω^* , is given in Eq. (8.7), and the corresponding optimal value of W is given in Eq. (8.8). The maximum in W , and therefore in power, is obtained for $\omega > \omega_0$ mostly since the effective detuning is $\widetilde{\Delta\omega}$ rather than $\Delta\omega$. The new “resonance condition,” $\widetilde{\Delta\omega} = 0$, is equivalent to

$$\omega_{\text{res}} = \omega_0 + \frac{(2\epsilon)^2}{\omega_0}. \quad (9.1)$$

The optimal frequency, ω^* , is shifted towards even higher frequency, by Γ_-^2/ω_0 . This is due to the fact that the effective amplitude, $\bar{\epsilon}$, in the numerator of Eq. (8.5), also depends on ω .

The normalized power is plotted as a function of ω in Fig. 13, for different values of the field amplitude. Figure 13 gives the characteristic line-shape function at the amplifier output. As ϵ increases, the field intensifies, and the line broadens. This is an effect similar to

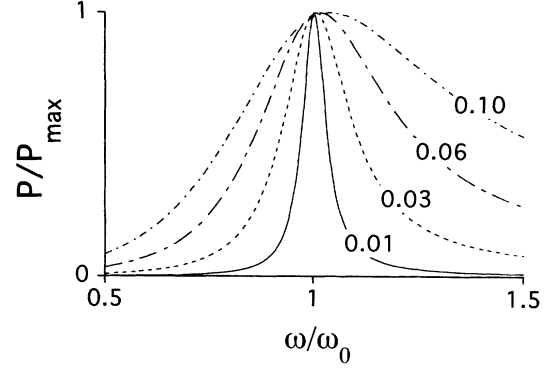


FIG. 13. The normalized power as a function of the field's frequency, ω (the line shape). The numbers on the curves correspond to the different values of the normalized field amplitude, ϵ/ω_0 . The parameters of the calculation are $T_c = 0.050$, $T_h = 0.500$, and $\mu = 0.001$.

power broadening in absorption spectra. Note that since the rate coefficients are field dependent the functional dependence of the line shape on the field amplitude is more complicated than that obtained in the standard theory.

C. Power optimization with respect to the field amplitude (ϵ)

The steady-state power is factorizable into three contributions [cf. Eq. (8.3)]. Each of the three factors depend on the field amplitude ϵ . The dependence of each term on ϵ was analyzed in Sec. VIII. The main conclusions are summarized:

(a) The first term is $E_1 - E_0$, the energy difference between the two upper field-shifted levels. It is a monotonically increasing function of ϵ . This term does not depend on the other parameters of the problem, except for ω_0 .

(b) The second term is W . It depends on all the parameters (T_c , T_h , μ , ω , ω_0 , and ϵ). Here, one should make a distinction between two cases. (1) When ω is constant, W has a maximum as a function of ϵ . The reason for this is that once the distance between the constant ω and the ϵ -dependent ω^* [Eq. (8.7)] increases, the amplifier gradually goes out of resonance [cf. Fig. 7], and the power diminishes. (2) When W is optimized with respect to ω for each value of ϵ , it is denoted by $W^*(\epsilon)$ [cf. Eq. (8.8)]. $W^*(\epsilon)$ is a monotonically increasing function of ϵ [cf. Fig. 8]. This is because the change in the resonance frequency, ω^* , is now followed as ϵ increases.

(c) The third term is a measure of population inversion, $\Pi_1^{ss} - \Pi_0^{ss}$ [Eq. (8.10)]. This term depends on all the parameters. It is maximal when $\epsilon = 0$ ($\Pi_1^{ss} - \Pi_0^{ss} \leq \Pi_1^0 - \Pi_0^0$), and reduces to zero as ϵ approaches ϵ_{max} . Thus a net decrease in the gain occurs as ϵ is increased. Since W appears in the denominator of the expression for the $\Pi_1^{ss} - \Pi_0^{ss}$, two possibilities must be distinguished: (1) When ω is fixed, $\Pi_1^{ss} - \Pi_0^{ss}$ will not decrease monotonically as ϵ increases. Instead it will go through a “bump”

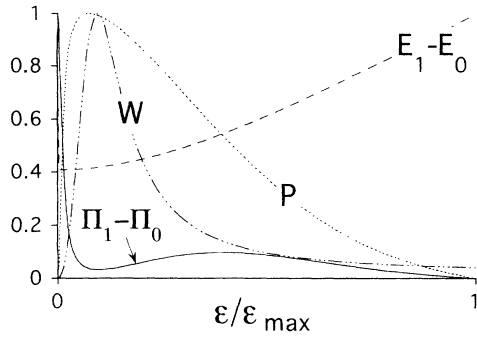


FIG. 14. The individual components contributing to the power as a function of the field amplitude ϵ , for fixed field frequency. Note the “bump” in the curve for $\Pi_1 - \Pi_0$. The components are normalized to their maximum. The parameters of the plot are $\omega_0 = 1.000$, $\mu = 0.005$, $\Delta\omega = 0.000$, $T_c = 0.050$, and $T_h = 0.500$.

as it decreases from $\Pi_1^0 - \Pi_0^0$ to zero (cf. Fig. 14). (2) When W is optimized with respect to ω , W^* becomes a monotonically increasing function of ϵ , and $\Pi_1^{ss} - \Pi_0^{ss}$ becomes a monotonically decreasing function of ϵ [cf. Fig. (11)].

The net decrease in $\Pi_1^{ss} - \Pi_0^{ss}$ as a function of ϵ is due to the fact that both pumping and cooling become less efficient as the energy splitting between the two upper field-shifted energy levels becomes larger [cf. Fig. (10)].

The above properties are summarized in Figs. 14 and 15. The power as a function of ϵ , obtained from the present model, is compared with that obtained in Lamb’s model, in Fig. 16. The predictions of both models coincide for low fields, as expected. However, the behavior in the high-field domain differs considerably. While in the field-dependent model the power has a maximum as a function of ϵ and reduces to zero at a finite field amplitude, it reaches saturation in Lamb’s model. This difference is the result of utilizing field-dependent dissipation, where the rate coefficients are explicitly dependent on the field amplitude ϵ . $\Pi_1^{ss} - \Pi_0^{ss}$ obtained in the field-dependent approach reduces to zero more quickly, and

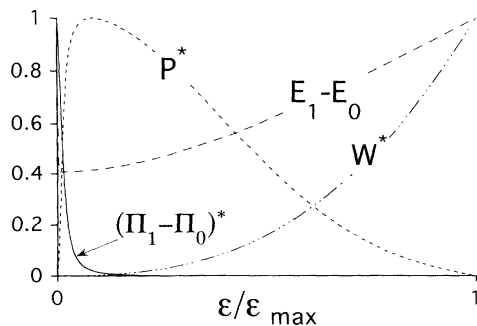


FIG. 15. The individual components contributing to the power, after optimization with respect to the field frequency, as a function of the field amplitude ϵ . The components are normalized to their maximum. The parameters of the plot are $\omega_0 = 1.000$, $\mu = 0.005$, $T_c = 0.050$, and $T_h = 0.500$.

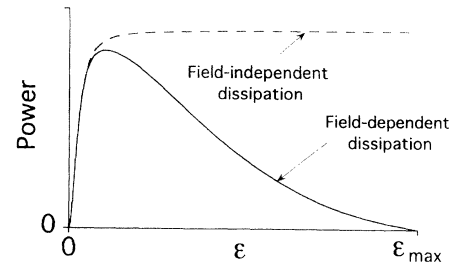


FIG. 16. Comparison of the power as a function of the field amplitude ϵ obtained in the present study with that obtained in the field-independent approach to dissipation (Lamb’s model). The comparison is made with the parameters $\omega_0 = 1.00$, $\mu = 0.01$, $\Delta\omega = 0.00$, $T_c = 0.05$, and $T_h = 0.50$.

becomes equal to zero at a finite value of ϵ . However, in the field-independent approach, the rate coefficients are field independent, and W is proportional to ϵ^2 , so that $\Pi_1^{ss} - \Pi_0^{ss}$ reduces to zero only asymptotically, like $1/\epsilon^2$.

The value of ϵ for which the power is optimized is denoted by ϵ^* . ϵ^* is a function of the temperatures. The power as a function of ϵ is plotted in Fig. 17 for different values of T_c (the temperature ratio is fixed and given by 0.1 in this case). The power function broadens as the temperatures increase and the maximum is shifted to higher amplitudes. Figure 17 is misleading since as the temperatures further increase ϵ^* moves backward to lower amplitudes. This can be seen in Fig. 18, where ϵ^* is plotted vs T_c for different values of T_c/T_h . The reverse in the direction in which ϵ^* moves, as seen on one of the curves, occurs in all the other curves at higher temperatures. This is probably due to the influence of dephasing which becomes increasingly important as the temperatures increase (cf. Sec. VIII). Since small amplitudes imply smaller dephasing, the engine is optimal for a smaller value of ϵ^* .

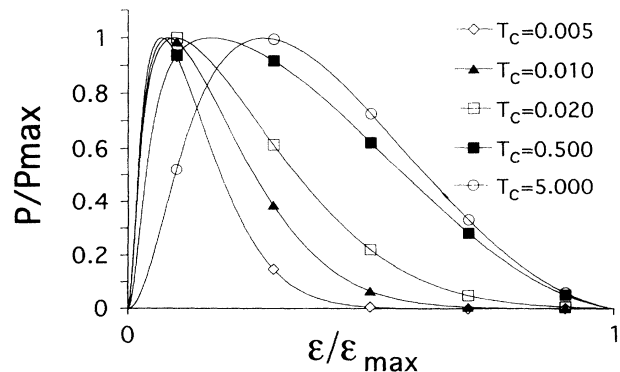


FIG. 17. The normalized power as a function of the normalized field amplitude for different temperatures. The temperature ratio is fixed: $T_c/T_h = 0.10$. The other parameters in this plot are $\omega_0 = 1.00$ and $\mu = 0.01$.

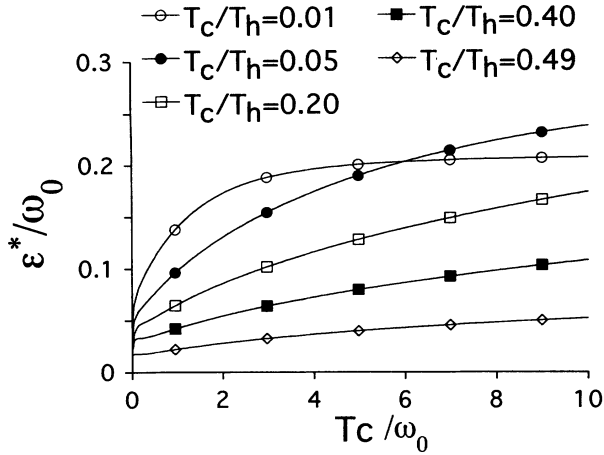


FIG. 18. The optimal normalized amplitude as a function of the normalized temperature of the cold reservoir. The parameters are $\omega_0 = 1.00$ and $\mu = 0.01$.

X. DISCUSSION

In the present work, thermodynamic consistency was utilized as the fundamental guide in the construction of quantum relaxation equations for a system subject to time-dependent external fields. It was shown that thermodynamic consistency requires that the relaxation terms become field dependent. Explicit simplified field-dependent relaxation equations were constructed for a three-level amplifier. The special interest in this system is due to the fact that it may be realized as a heat engine. The steady-state solution of these equations was found to be considerably different in comparison with that obtained from the standard theory, where the relaxation is assumed to be field independent. The deviations are most pronounced for intense fields. Their most important manifestations were found to be the following.

(a) The steady-state power production has a maximum as a function of the field amplitude. In contrast to the steady-state power obtained from the standard theory which saturates as the field intensifies.

(b) The “resonance frequency,” i.e., the frequency for which the transition probability, and therefore the power production, are maximized, is field dependent. The resonance frequency in the standard theory is just $\omega = \omega_0$.

Utilizing consistent definitions of thermodynamical quantities in terms of quantum expectation values, a finite-time thermodynamic analysis of the quantum engine was carried out. The power production was chosen to be the target for optimization. It was maximized with respect to the field’s amplitude and frequency, the coupling parameter, and the temperatures of the heat reservoirs. It was demonstrated how quantum phenomena, such as the splitting of energy levels by the field and dephasing, can be visualized as sources for losses from the point of view of finite-time thermodynamics.

The main drawbacks of the present work are the field-dependent relaxation equations, which were constructed rather than derived. The underlying principle of the con-

struction is to obtain the simplest relaxation dynamics which satisfy consistency with thermodynamics. Such an approach undoubtedly leaves out some of the physics (cf. Sec. VII). However, this simple model already gives predictions that considerably deviate from those of the standard field-independent theory. Furthermore, the physical origin of these deviations is clear, and seems to be more general than the specific model used. An alternative and more rigorous approach would be to derive the field-dependent relaxation equations in the weak coupling limit. The results of such an approach will be described in a future publication. It will come as no surprise, however, that the equations obtained in such an approach are far more difficult to work with and interpret.

The working medium in the model consists of atoms with equally spaced energy levels. This assumption was made only for the sake of simplicity. When generalized to atoms with arbitrary level spacing, general trends found in the present study remain qualitatively valid. It should also be noted that once the constraint on the energy spacing is removed they become admissible controls [3,4]. The limit where both power and efficiency are zero, the “short-circuit” limit, can then be obtained.

The present study has many similarities to the previous model of a continuous heat engine constructed from two harmonic oscillators of frequencies ω_a and ω_b [5]. The work reservoir in that model consisted of a rotating field of the resonance frequency $\nu = \omega_a - \omega_b$. It was found there that in order to obtain thermodynamic consistency the relaxation terms had to be field dependent. In both Ref. [5] and the present study, field-dependent relaxation equations were constructed, rather than derived, following the basic demand of consistency with thermodynamics. In both cases that demand led to the assumption of instantaneous detailed balance.

The other manifestation of the field’s presence is the mixing of eigenstates coupled by the field. In the present work, this effect was dealt with by using creation and annihilation operators based upon the instantaneous, mixed, energy eigenstates. In Ref. [5], however, relaxation terms of the general semigroup type, mixing the creation operator of one dressed normal mode with the annihilation operator of the other, were utilized. The main difference between the two approaches is made clear when one of the heat reservoirs, say the cold reservoir, is decoupled. In such a case, the system will asymptotically approach different stationary states: The two dressed normal modes in Ref. [5] reach thermal equilibrium with the hot reservoir, while in the three-level atom of the present work the populations in $|E_{-1}\rangle$ and $|E_1\rangle$ reach thermal equilibrium with the hot reservoir and the population in $|E_0\rangle$ is equal to that in $|E_1\rangle$.

The asymptotic behavior in Ref. [5] is what one would expect from a system with stationary internal coupling, where only one part of the system is directly interacting with the heat reservoir [23]. However, the coupling in the present study is explicitly time dependent, unless the field is included in what is defined as “the system.” To rigorously do this, one has to treat the field as a quantum entity, which is not done in Ref. [5]. The remedy to this seeming contradiction is found in using the dressed-state

picture, which is only adequate in resonance (which is why $\nu = \omega_a - \omega_b$ in Ref. [5]). It is interesting to note that the field is considered part of the system for the description of the coupling with the field, while the relaxation of the field by the heat reservoir is neglected. The point of view adopted in the present work differs from that of Ref. [5] by the fact that the field is never considered as part of the system. The asymptotic state of the system, as opposed to the dressed system in Ref. [5], is then easy to comprehend if the external field is considered as a work reservoir of infinite temperature [7]: The two-level subsystems $\{|E_{-1}\rangle, |E_1\rangle\}$ and $\{|E_0\rangle, |E_1\rangle\}$ reach thermal equilibria corresponding to the temperatures T_h and ∞ , respectively.

The problem addressed in the present study belongs to a larger class of processes subject to time-dependent external constraints while performing thermal relaxation. This topic was avoided to a large extent in the literature. However, such processes are of fundamental importance in thermodynamics, spectroscopy, and quantum optics. In this study the use of thermodynamical criteria has been found to be crucial in the analysis. However, the field-dependent relaxation theory obtained by only using thermodynamical criteria is incomplete. A complete theory would require a rigorous derivation of the relaxation equations in the presence of the field. This topic is currently under study.

ACKNOWLEDGMENTS

We wish to thank Professor J. L. Skinner, Professor R. Silbey, Professor K. R. Wilson, and their groups for

their helpful comments and hospitality. We also thank the participants of the workshop on thermodynamics of complex systems held at the Telluride Summer Research Center for stimulating discussions. This research was supported by the Israel Science Foundation administered by the Israel Academy of Science. The Fritz Haber Research Center is supported by the Minerva Gesellschaft für die Forschung, GmbH München, FRG.

APPENDIX: THE EFFECT OF MIXING IN THE GENERAL CASE

Consider, for example, the coupling of the levels $|-1\rangle$ and $|1\rangle$ to the hot reservoir. The most general reservoir-system couplings have the following form:

$$\mathbf{H}_{RS} = \mathcal{G} \otimes \mathbf{P}_{1,-1} + \mathcal{G}^\dagger \otimes \mathbf{P}_{-1,1} + \mathcal{D} \otimes (\mathbf{P}_1 - \mathbf{P}_{-1}), \quad (\text{A1})$$

where \mathcal{G} , \mathcal{G}^\dagger , and \mathcal{D} are observables of the hot reservoir. The coupling with the field mixes the states $|1\rangle$ and $|0\rangle$ to give the new eigenstates $|E_1\rangle$ and $|E_0\rangle$ ($|E_1\rangle$ is assumed higher in energy than $|E_0\rangle$). The hot reservoir is now supposed to relax the two-level system $|E_1\rangle$ and $|-1\rangle$. However, the two-dimensional sub-space spanned by $|-1\rangle$ and $|1\rangle$ does not coincide with the two-dimensional subspace spanned by $|-1\rangle$ and $|E_1\rangle$. Thus one cannot write \mathbf{H}_{RS} in terms of the eigenprojectors of the subspace spanned by $|-1\rangle$ and $|E_1\rangle$, and one must treat the coupling to the hot reservoir in terms of a three-level system rather than a two-level system. The same conclusion is true for the coupling with the cold reservoir.

-
- [1] S. Carnot, *Réflexions sur la Puissance Motrice du Feu et sur les Machines propres à Développer cette Puissance* (Bachelier, Paris, 1824).
 - [2] For a survey of the field's present state see *Finite Time Thermodynamics and Thermoconomics*, Advances in Thermodynamics Vol. 4, edited by S. Sieniutycz and P. Salamon (Taylor & Francis, London, 1991), and references therein.
 - [3] E. Geva and R. Kosloff, *J. Chem. Phys.* **96**, 3054 (1992).
 - [4] E. Geva and R. Kosloff, *J. Chem. Phys.* **97**, 4398 (1992).
 - [5] R. Kosloff, *J. Chem. Phys.* **80**, 1625 (1984).
 - [6] C.P. Slichter, *Principles of Magnetic Resonance* (Springer-Verlag, Berlin, 1978).
 - [7] J.E. Geusic, E.O. Schultz-du Bois, R.W. De Grasse, and H.E.D. Scovil, *J. Appl. Phys.* **30**, 1113 (1959); H.E.D. Scovil and E.O. Schultz-du Bois, *Phys. Rev. Lett.* **2**, 262 (1959); J.E. Geusic, E.O. Schultz-du Bois and H.E.D. Scovil, *Phys. Rev.* **156**, 343 (1967); R.D. Levine and O. Kafri, *Chem. Phys. Lett.* **27**, 175 (1974); R.D. Levine and O. Kafri, *Chem. Phys.* **8**, 426 (1975); A. Ben-Shaul and R.D. Levine, *J. Non-Equilib. Thermodyn.* **4**, 363 (1979).
 - [8] W.H. Louisell, *Quantum Statistical Properties of Radiation* (Wiley, New York, 1990).
 - [9] H.B. Callen, *Thermodynamics* (Wiley, New York, 1979).
 - [10] R. Alicki and K. Lendi, *Quantum Dynamical Semigroups and Applications* (Springer-Verlag, Berlin, 1987).
 - [11] L. Allen and J. Eberly, *Optical Resonance and Two-Level Atoms* (Dover, New York, 1987).
 - [12] H. Spohn and J.L. Lebowitz, *Adv. Chem. Phys.* **38**, 109 (1979).
 - [13] R. Alicki, *J. Phys. A* **12**, L103 (1979).
 - [14] E.B. Davies, *Quantum Theory of Open Systems* (Academic, New York, 1976).
 - [15] A. Abragam, *The Principles of Nuclear Magnetism* (Clarendon, Oxford, 1961).
 - [16] C. Cohen-Tannoudji, *Atom-Photon Interactions* (Wiley, New York, 1992).
 - [17] G. Lindblad, *Commun. Math. Phys.* **48**, 119 (1976).
 - [18] V. Gorini, A. Kossakowski, and E.C.G. Sudarshan, *J. Math. Phys.* **17**, 821 (1976).
 - [19] F. Bloch, *Phys. Rev.* **70**, 460 (1946).
 - [20] B.B. Laird, J. Budimir, and J.L. Skinner, *J. Chem. Phys.* **94**, 4391 (1991).
 - [21] W.E. Lamb, Jr., *Phys. Rev.* **134**, A1429 (1964).
 - [22] A.G. Redfield, *IMB Jr.* **1**, 19 (1957).
 - [23] H.J. Carmichael and D.F. Walls, *J. Phys. A* **6**, 1552 (1973).

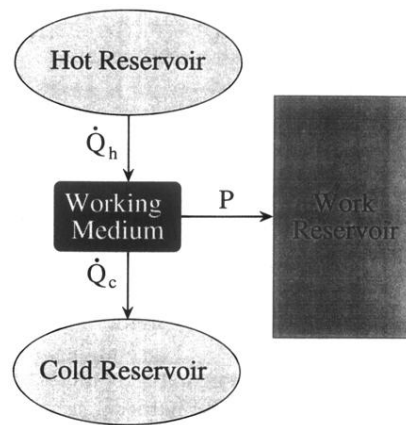


FIG. 1. The generic heat engine. The arrows indicate the directions of the heat and work currents.